

# Destructuration of soft clay during Shield TBM tunnelling and its consequences

Hirokazu Akagi

**Abstract** It is very important to prevent ground settlement associated with shield TBM tunnelling in soft ground in order to avoid the damage to existing superstructures in urban area. However, consolidation settlement takes place in the surrounding ground under its own weight due to soft clay destructuration with the decrease of effective stress, since it is inevitable that the adjacent clay suffers the undrained shear deformation during shield TBM tunnelling within soft clay ground. Such consolidation phenomena of normally consolidated soft clays due to their destructuration are investigated. It is concluded from experiments and theoretical investigation that the volume decrease of normally consolidated soft clays necessary to predict the ground subsidence behavior is obtained by using the magnitude of shear strain during undrained shear deformation and clay sensitivity and plasticity index, which are related to the susceptibility to soft clay destructuration.

## 1 Introduction

The shield TBM tunnelling method is frequently used for constructing the underground structures for railways and utility lines in urban area. The method has been employed extensively for more than 40 years, and many advances - such as the development of new excavation machines and the implementation of computer controlled operation - have been made in order to optimize the method. Based on the large amount of experience and expertise, the sources of ground deformation associated with shield TBM tunnelling are well investigated. In recent years, the magnitude of soil deformation by earth pressure balance shield TBM tunnelling in soft ground has become remarkably small: surface settlements of less than 10 mm are common.

---

Hirokazu Akagi  
Waseda University, Ohkubo3-4-1-58-205, Shinjuku, Tokyo, Japan, e-mail: akagi@waseda.jp

Even with recent advances in the method, shield TBM tunnelling in soft clay, where the  $N_{SPT}$  value is close to zero, is still a major technical challenge for tunnel engineers. Deformation in this type of soil tends to occur several months or years after the completion of tunnelling. This long term settlement is due mainly to consolidation of soft clay around the tunnel, originating from the excess pore water pressure generated from the destructuration of soft clay during the shield TBM tunnelling, as the soft clay is subjected to the shear deformation during the cutting at the TBM face, the TBM advancement and the tail void deformation behind the TBM.

In this paper, such consolidation phenomena of normally consolidated soft clays due to their destructuration are investigated and it is concluded from experiments and theoretical considerations that the volume decrease of normally consolidated soft clays necessary to predict the ground subsidence behavior is obtained by using the magnitude of shear strain during undrained shear deformation, clay sensitivity, and plasticity index, which related to the susceptibility to clay destructuration.

## 2 Field settlement records

Figs. 1 and 2 demonstrate the field measurement results of vertical settlement distribution of soft soil observed at about 6 months after the completion of twin shield TBM tunnelling at Tokyo around 1970s. Both the magnitude of vertical settlement observed at the central axes and the side positions of tunnels and the magnitude of ground loss obtained from the area of the settlement trough at some depth become greater at the shallower depth. This means that the consolidation settlement takes place and accumulates within the silt layer above the tunnels and the magnitude of vertical settlement at some depth is increased by the volume decrease of silt soil. The physical properties of silt soil are as follows. The plasticity index values of silt soil is low, i.e. around 10 - 20 and the natural water content is greater than the liquid limit, i.e. the sensitivity value is quite large, i.e. around 20-40.

The displacements and strains of soft soil associated with shield TBM tunnelling are assumed to be great enough to break the bonds between particles and change their microstructure, i.e. destructuration as Peck suggested (1969) [2]. Hence, the zone of soil with destructuration can be created surrounding the tunnel and delayed consolidation settlement of the ground surface will take place owing to consolidation of destructured soil.

The mechanism of this consolidation of soft soil due to its disturbance, i.e. destructuration is illustrated as follows. In Fig. 3, typical oedometer test results of soft soils are shown for undisturbed soil *a*, slightly disturbed soil *b* and completely remolded soil *c*.

If shield TBM is driven in soft soil corresponding to the normally consolidated state at point (1) on undisturbed line *a*, the soft soil adjacent to the tunnel will be disturbed under constant void ratio. The state of this soil will move to point (2) on line *b*, since the effective stress decreases to  $\sigma'_r$  due to soil destructuration. The state

of total stress acting on the surrounding soil is assumed to recover the initial  $K_0$  condition at rest gradually after the passage of shield TBM. Therefore, the effective

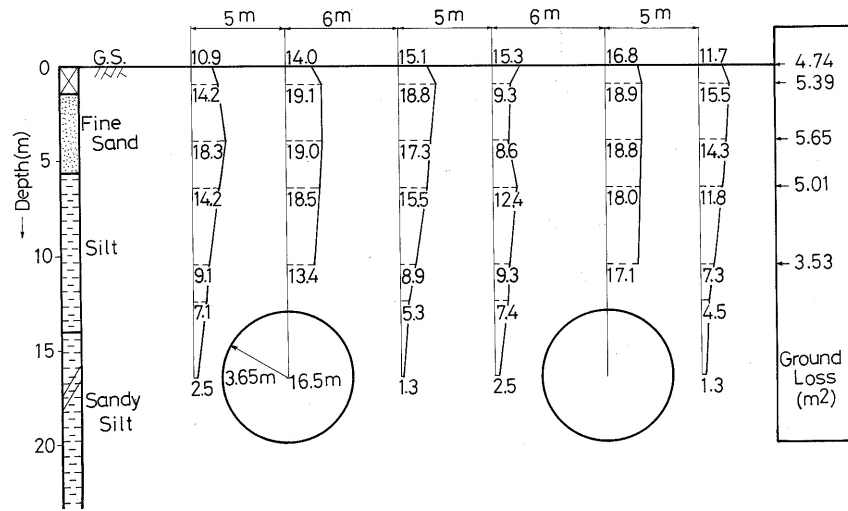


Fig. 1: Field measurement records at site 1

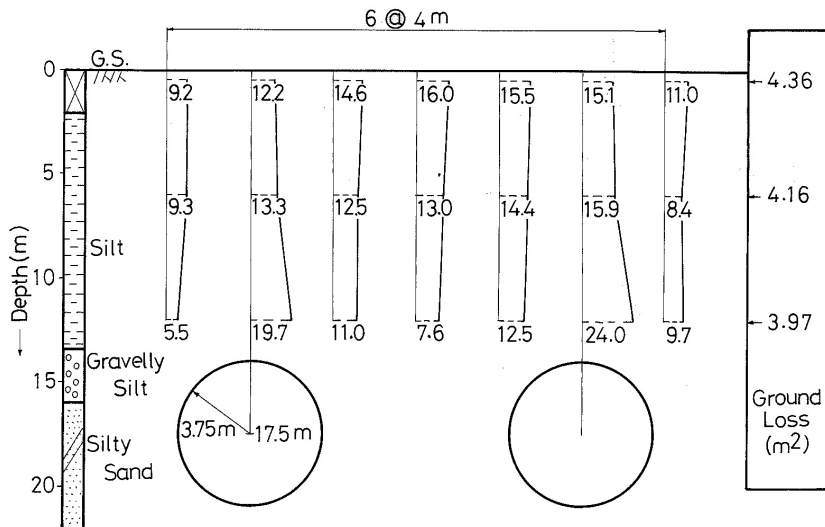
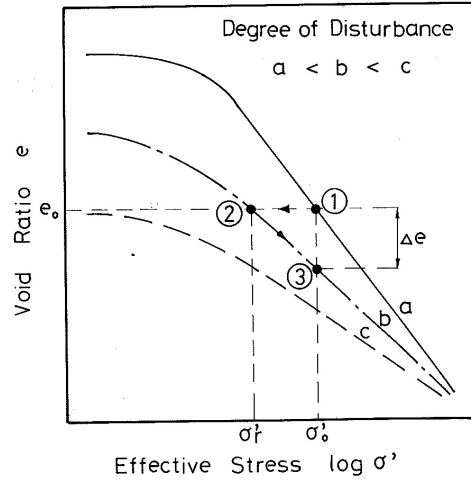


Fig. 2: Field measurement records at site 2



**Fig. 3** Typical oedometer test result of soft soil

stress increases up to  $\sigma'_0$  along line b and the state of soil will arrive at the point (3). In other words, the void ratio of the soil decreased by  $\Delta e_0$  under constant effective overburden pressure  $\sigma'_0$  and the consolidation of disturbed soil can take place.

### 3 Experimental investigation and discussion

Disturbance, i.e. destructure of soft soil is defined as the decrease of effective stress derived from the change of clay structure, which means the collapse of solid contacts between peds (or aggregates of clay platelets) and coarser particles by shear deformation under constant total stress condition. The disturbance ratio  $R$  defined as the change of effective stress is adopted as the measure of clay disturbance, for the change of mechanical characteristics of clays due to their disturbance is essentially caused by the change of effective stress. The disturbance ratio  $R$  or its increment  $r$  is defined by Eq. (1).

$$R = \sigma'_0 / \sigma'_r, \quad r = R - 1 = (\sigma'_0 - \sigma'_r) / \sigma'_r \quad (1)$$

in which  $\sigma'_0$ ; effective stress at undisturbed state (corresponding to the initial isotropic consolidation effective stress in the experiments described later),  $\sigma'_r$ ; residual effective stress at disturbed state to some degree.

However, it is assumed that the unique relationship should exist between this disturbance ratio  $R$  and the magnitude of shear strain  $\gamma_{oct}$ , because clay disturbance is originally derived from the change of clay structure by shear deformation. And it is reasonable to evaluate the disturbance ratio from the magnitude of ground displacement or shear strain comparatively easily obtained, for example, by finite element

analysis, since it is difficult to predict directly the change of effective stress (or excess pore water pressure in saturated clay), when the change of total stress condition is indeterminate. So the relationship between the disturbance ratio  $R$  and the magnitude of shear strain  $\gamma_{oct}$  during undrained shear stress loading is deduced according to the Anisotropic Cam Clay model, [1] in the case of undrained shear stress loading and unloading on isotropically normally consolidated soft soil as in the experiments described later and represented by Eq. (2).

$$R = \exp(A - (1 - \exp(-B \cdot \gamma_{oct})))$$

$$A = 1 - (\kappa/\lambda)^2, \quad B = 3\lambda/\kappa \cdot \mu$$
(2)

in which  $\gamma_{oct}$ : octahedral shear strain,  $\lambda$ : compression index,  $\kappa$ : swelling index,  $\mu$ : dilatancy constant.

Using this  $R$  versus  $\gamma_{oct}$  relationship,  $R$  can be obtained from the magnitude of shear strain during undrained shear, but this may be approximated as linear relationship until the magnitude of shear strain attains to 1.5% as shown in Fig. 4. So the relationship between  $r = R - 1$  and is assumed to be given by Eq. (3).

$$r = R - 1 = k' \cdot \gamma \quad \text{or} \quad r = k \cdot \gamma$$
(3)

The constant  $k$  contained in Eq. (3) is the soil parameter related to the susceptibility to soil disturbance, which controls the magnitude of  $r$  in the case of suffering given magnitude of shear strain, dependent on soil type or difference in soil structure.

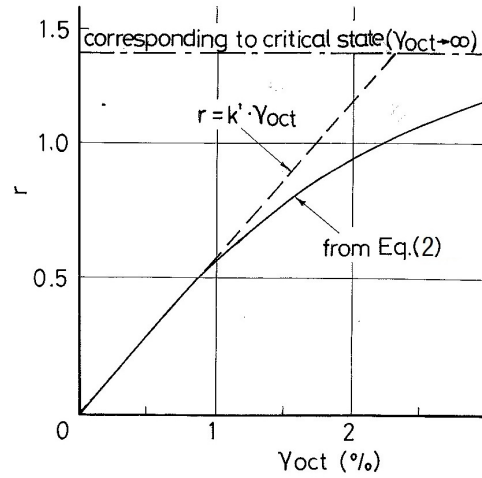


Fig. 4: Relationship between the increment of disturbance ratio  $r$  and the magnitude of shear strain  $\gamma_{oct}$  during undrained shear stress loading.

It is assumed that consolidation phenomena of normally consolidated soft soils due to such disturbance can occur when effective stress once decreased to  $\sigma'_r$  at disturbed state to some degree increases up to  $\sigma'_0$  at initial state under its own weight. In this case, volume decrease of soft soil  $\alpha$  can be represented by using the magnitude of shear strain  $\gamma$  as in Eq. (4).

$$\begin{aligned}\alpha &= (C'_c/(1+e_0)).\log R \\ &= (C'_c/(1+e_0)).\log(k.\gamma+1)\end{aligned}\quad (4)$$

in which  $e_0$  is the initial void ratio before undrained shear and  $C_c$  is the compression index of disturbed clay during the reconsolidation process, as shown in Fig. 5. As it

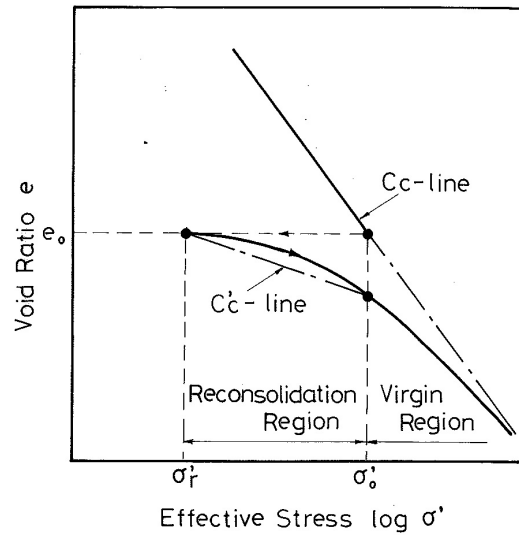


Fig. 5: Schematic diagram of the consolidation phenomena of normally consolidated clays due to the disturbance caused by undrained shear.

is considered that soft soil disturbance is influenced by type of soil or difference in soil structure, three types of undisturbed samples used in the experiments ( $S_r=12.5-45.4$ ) were prepared by sampling soil blocks obtained from three construction sites in Tokyo area. Other five samples were prepared by mixing and reconsolidating the alluvial clay and Toyoura sand having four different mixing ratios ( $I_p=3.7-24.9$ ) and commercial clay ( $I_p=44.3$ ) in order to investigate the influence of the value of plasticity index on soil disturbance. Sample properties are listed in Table 1. Cylindrical specimens (50 mm in diameter and 110 mm in height) trimmed from these block samples were consolidated under isotropic stress  $\sigma'_0$  greater than the consolidation yield stress. The undrained triaxial compression tests were performed to give dif-

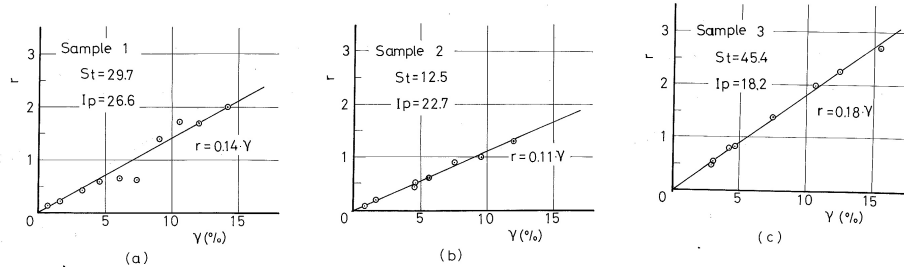


Fig. 6: Relationships between the increment of disturbance ratio  $r$  and magnitude of shear strain  $\gamma$  during undrained shear stress loading.

ferent magnitudes of shear strain up to 10% axial strain to soil specimens and shear stress was gradually unloaded under undrained condition, until the initial isotropic stress state was recovered.

Then, pore-water pressure values at that state  $\Delta u_r$  were measured and soil specimens were consolidated again under the same isotropic stress condition as in the initial consolidation. In this way, the relationships between the change of effective stress or the volume decrease of specimens due to clay disturbance and the magnitude of shear strain during undrained shear stress loading were investigated.

According to these test results, the increment of disturbance ratio  $r$  versus shear strain  $\gamma$  relationships are shown in Figs. 6 (a), (b), and (c). It is clear from these figures that linear relationships exist between  $r$  and  $\gamma$  also in the range of the magnitude of shear strain greater than the value corresponding to  $\gamma_{oct} = 1.5\%$ . The parameter  $k$  related to the susceptibility to soil disturbance, corresponding to the gradient of  $r$  versus  $\gamma$  relationship is different for each sample. Parameter  $k$  is greater for undisturbed samples having greater clay sensitivity and the value of plasticity index is smaller. The parameter  $k$  is assumed to be represented by Eq. (5) as the function of clay sensitivity  $S_t$  and the value of plasticity index  $I_p$ .

$$k = 0.33 \cdot I_p^{-0.37} \cdot \log S_t \quad (5)$$

In Fig.7, parameter  $k$  obtained from these test results are plotted on semi-logarithmic chart  $k$  versus  $S_t$  as the function of  $I_p$ . Compression index of disturbed clay during

Table 1: Sample property

Sample	1	2	3	A	B	C	D	E
Ip	26.6	22.7	18.2	3.7	8.6	15.2	24.9	44.3
St	29.7	12.5	45.4	4.2	4.6	4.8	5.9	4.0
Parameter k	0.14	0.11	0.18	0.13	0.10	0.080	0.074	0.054

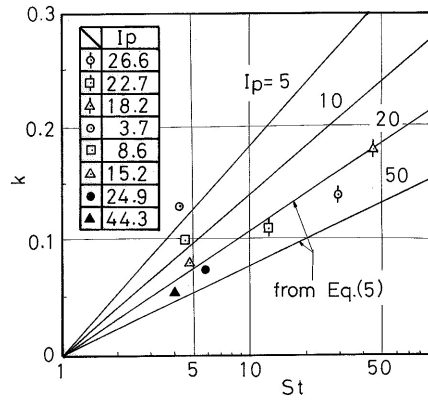


**Fig. 7** Relationship between parameter  $k$  and clay sensitivity  $S_t$  in function of  $I_p$ .

the reconsolidation process  $C'_c$  is also investigated by using the test results. Figure 8 shows the compression index ratio  $C'_c/C_c$  ( $C_c$ ; compression index at undisturbed state) versus the increment of disturbance ratio  $r$ .  $C'_c$  decreases with  $r$  and its way of decrease is different for undisturbed samples and for remolded ones. But it is assumed to be convenient to use constant value of  $C'_c$  value for undisturbed samples and for remolded ones, since  $C'_c$  value decreases rapidly in the region of small  $r$  value and thereafter may be almost constant.

$$\begin{aligned} C'_c &= 0.3C_c && \text{For undisturbed samples} \\ C'_c &= 0.6C_c && \text{For remolded samples} \end{aligned} \quad (6)$$

Using these constants  $k$  and  $C'_c$  in Eq. (4),  $\alpha$  can be obtained from the magnitude of shear strain  $\gamma$  during undrained shear stress loading. For example,  $\alpha$  versus  $\gamma$  relationships are shown in Figs.9.(a), (b) and (c).

#### 4 Numerical simulation of consolidation settlement due to soil destructuration during shield TBM tunnelling

Numerical simulation of consolidation settlement has been conducted by using the relationship  $\alpha$  and  $\gamma$  obtained from the experimental results and theoretical approach. Fig. 10 shows the 2-D finite element mesh employed to obtain the shear strain distribution around the tunnel due to the stress release at the tail void behind the TBM, assuming the symmetrical distribution of shear strain with regard to the tunnel axis. Table 2 shows the input parameters for the elastic finite element analysis. Fig.11 indicates the shear strain distribution obtained from the 2D finite element analysis. The shear strain extends to the upward diagonal direction from the tunnel.

In order to obtain the magnitude of consolidation settlement, the following proce-

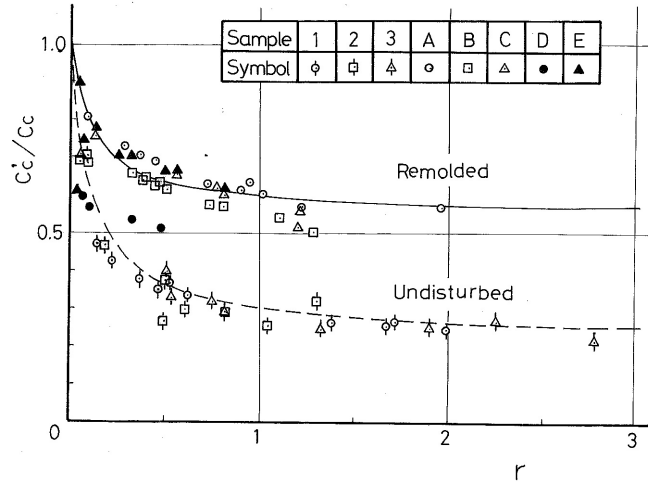


Fig. 8: Relationship between compression index ratio  $C'_c/C_c$  and the increment of disturbance ratio  $r$ .

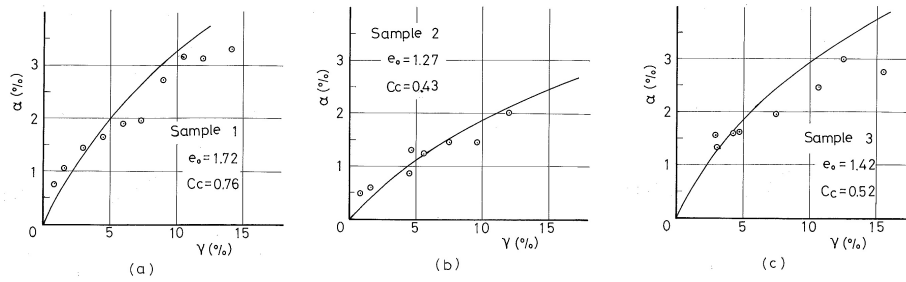


Fig. 9: Relationship between the volume decrease  $\alpha$  due to clay and the magnitude of shear strain  $\gamma$  during undrained shear stress loading.

ture has been used. The input parameters for the calculation of  $\alpha$  are as follows:  $C'_c=0.18$ ,  $e_0=1.50$ ,  $S_t=20$ ,  $I_p=20$ .

1) The area separated by the equi-shear strain lines greater than  $\gamma=1(\%)$  is divided into the small pieces of blocks as shown in Fig.12.

2) In the case of block A in Fig.12, the volume decrease  $\alpha=0.00316$  due to the soil destructuration is given by Eq.(4). Then, the height reduction  $S_A$  of this block A associated with  $\alpha$  is given as follows.

$$S_A = \frac{\alpha \cdot V_A}{2 \cdot I_A} \quad \text{in which } V_A \text{ is volume of block A} \quad (7)$$

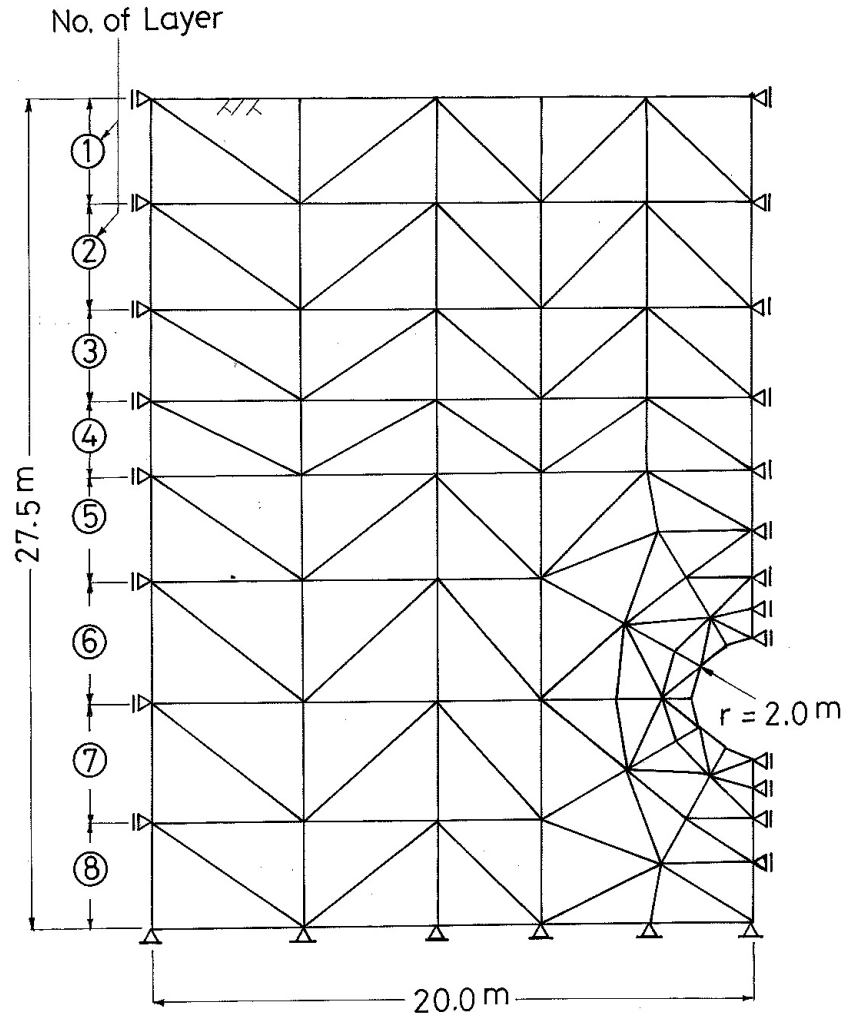


Fig. 10: 2D Finite Element mesh used in the simulation

3) The height reduction  $S_A$  of block A induces the ground settlement  $\delta_A$ , assuming the exponential distribution of the settlement trough at the depth  $z$ .  $\delta_A$  is given by the following equations.

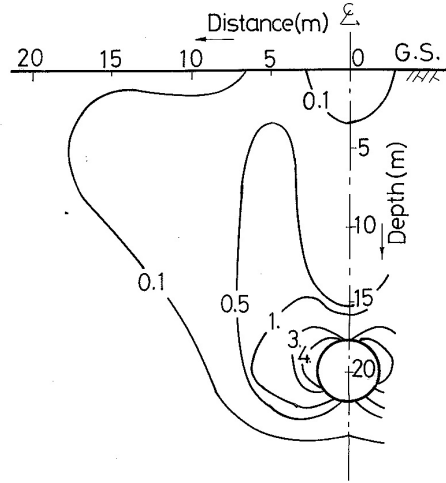


Fig. 11: Shear strain distribution around the tunnel

$$i) 0 \leq x_A \leq l_A;$$

$$\sigma_A = \frac{S_A}{2} \cdot (\sqrt{1 - \exp(-\frac{1}{2} \cdot X_1^2)} + \sqrt{1 - \exp(-\frac{1}{2} \cdot X_2^2)})$$

$$ii) x_A > l_A;$$

$$\sigma_A = \frac{S_A}{2} \cdot (\sqrt{1 - \exp(-\frac{1}{2} \cdot X_1^2)} - \sqrt{1 - \exp(-\frac{1}{2} \cdot X_2^2)}) \quad (8)$$

in which

$$X_1 = \frac{x_A + l_A}{\sigma_A}, \quad X_2 = \frac{x_A - l_A}{\sigma_A}$$

$$\sigma_A = \frac{L_A}{2.13}, \quad L_A = H_A + l_A - Z$$

Table 2: Input parameters for Finite Element calculation

No. of Layer	Undrained Shear Strength $C_u$ (tf/m <sup>2</sup> )	Initial Tangent Modulus $E_i$ (tf/m <sup>2</sup> )	Poisson's ratio $\nu$	Unit Weight $\gamma$ (tf/m <sup>3</sup> )	Earth Press. coeff. at rest $K_0$
1	1.26				
2	1.26				
3	2.04				
4	2.07				
5	3.42	84.0	0.485	16.0	0.80
6	4.32				
7	5.28				
8	6.18				

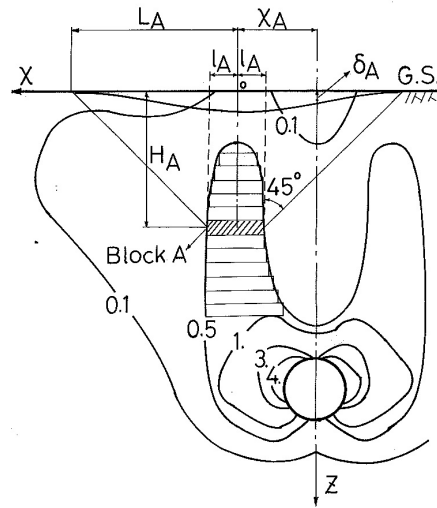


Fig. 12: Calculation procedure for consolidation settlement

4) The calculation procedure mentioned above is repeated for all the blocks within the shear strain distribution and summed up.

Fig.13 shows the vertical consolidation settlement distribution along the tunnel axis and the side position from 4(m) apart from the axis. The magnitude of vertical settlement becomes greater at the shallower depth, since the consolidation settlement is added from the volume decrease  $\alpha$  of the soft soil with destructuration.

## 5 Concluding remark

In this paper, the characteristic settlement distribution due to the shield TBM tunnelling within the soft soil has been indicated. The consolidation of soft soil due to the destructuration associated with shield TBM has been investigated experimentally and theoretically. Numerical simulation of consolidation settlement has reproduced the settlement distribution similar to the measurement results at the shield TBM tunnelling within the soft soil.

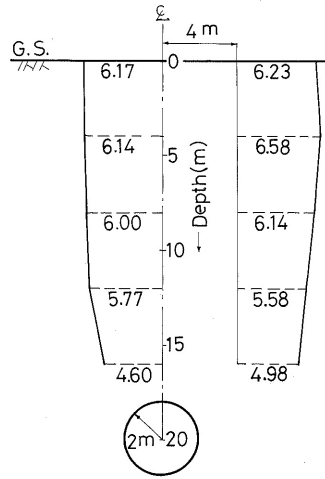


Fig. 13: Vertical consolidation settlement distribution along, and side of the tunnel

## References

1. Ohta, H., S.Yoshitani and S.Hata: *Anisotropic stress-strain relationship of clay and its application to finite element analysis*, Soils and Foundations, Vol.13, No.4, pp.61-79, 1975.
2. Peck, R. B. *Deep excavation and tunnelling in soft ground, State of the art report*, 7th IC-SMFE, pp.225-290, Mexico, 1969.